

A study of the first-order valence transition in  $\text{Ce}(\text{Ni}_{1-x}\text{Co}_x)\text{Sn}$  single crystals by magnetic susceptibility measurements

This article has been downloaded from IOPscience. Please scroll down to see the full text article.

1999 J. Phys.: Condens. Matter 11 543

(<http://iopscience.iop.org/0953-8984/11/2/017>)

View [the table of contents for this issue](#), or go to the [journal homepage](#) for more

Download details:

IP Address: 171.66.16.210

The article was downloaded on 14/05/2010 at 18:30

Please note that [terms and conditions apply](#).

## A study of the first-order valence transition in Ce(Ni<sub>1-x</sub>Co<sub>x</sub>)Sn single crystals by magnetic susceptibility measurements

D T Adroja<sup>†</sup>, Y Echizen<sup>†</sup>, T Takabatake<sup>†</sup>, Y Matsumoto<sup>†</sup>, T Suzuki<sup>†</sup>,  
T Fujita<sup>†</sup> and B D Rainford<sup>‡</sup>

<sup>†</sup> Department of Quantum Matter, ADSM, Hiroshima University, Higashi-Hiroshima 739-8526,  
Japan

<sup>‡</sup> Department of Physics, Southampton University, Southampton SO17 1BJ, UK

Received 11 September 1998, in final form 28 October 1998

**Abstract.** The first-order valence transition in CeNi<sub>1-x</sub>Co<sub>x</sub>Sn has been investigated for single crystalline samples with  $x = 0.32$  and  $x = 0.35$  as well as for polycrystalline samples with  $0.31 \leq x \leq 0.38$  ( $x$  varied in steps of 0.01) through the measurements of magnetic susceptibility,  $\chi$ . For the single crystal with  $x = 0.32$ ,  $\chi(T)$  exhibits a strong anisotropic mixed-valence behaviour. On the other hand,  $\chi(T)$  of the crystal with  $x = 0.35$  exhibits a sharp first-order valence transition at 50 K. In both crystals, the strong anisotropy,  $\chi_a > \chi_b \approx \chi_c$ , is maintained as in the host compound CeNiSn. The arc-melted polycrystalline alloys with a narrow range of Co composition,  $x = 0.33$ – $0.37$ , show a sharp drop in  $\chi(T)$  below 70 K and large hysteresis. This transition becomes sharper by annealing at 1000 °C. For the optimum concentration  $x = 0.35$ , the drop in  $\chi(T)$  at the transition becomes as high as 72% for the single crystal and 69% for the polycrystalline alloy for which a jump in ac heat capacity was observed at 55 K. Analysis of the above results reveals that the phase transition involves a large change in the Kondo temperature  $\Delta T_K/T_K = 11.2$ . The small volume discontinuity  $\Delta V/V = -0.003$  at the transition suggests that the phase transition is not due to a Kondo volume collapse. A possible mechanism responsible for the phase transition in the present alloys is proposed.

### 1. Introduction

Many Ce- and Yb-based intermetallic compounds display intermediate valence (IV) or non-integral valence behaviour [1–5]. This behaviour arises due to the presence of nearly degenerate  $4f^n$  and  $4f^{n+1}$  configurations, where  $n$  is the number of electrons in the 4f shell. Generally the intermediate valence systems exhibit a gradual change in the valence of rare-earth ions with temperature, pressure and alloying [4–7]. This behaviour of IV systems could be well understood by invoking the presence of strong hybridization between 4f electrons and conduction electrons. However, there exists only a handful of systems in which the valence transition is of first order as a function of temperature or pressure and the crystal symmetry remains the same below and above the transition. This first-order transition is characterized by a latent heat, a finite change in unit-cell volume and hysteresis in the physical properties.

The rare-earth compounds exhibiting temperature or pressure induced first-order valence transitions are: Ce metal which shows the  $\alpha \rightarrow \gamma$  phase transition as the pressure rises to 8 kbar at room temperature [8], CeNi [9], Sm<sub>1-x</sub>Gd<sub>x</sub>S [10], a few Eu-based intermetallics [11, 12], YbInCu<sub>4</sub> [13] and very recently discovered alloys CeNi<sub>1-x</sub>Co<sub>x</sub>Sn ( $x = 0.35$ – $0.38$ ) [14]. The

$\alpha \rightarrow \gamma$  phase transition can also be induced as a function of temperature at ambient pressure in an alloyed system  $\text{Ce}_{1-x}\text{Th}_x$  [15]. Depending upon the Th concentration the transition can be first order, second order or continuous [15].

Theories of first-order valence transition are not well developed as those of continuous phase transitions. The  $\alpha \rightarrow \gamma$  phase transition has received considerable attention throughout the years and several models have been proposed to explain the phenomenon. The most well known are the promotional model [16], the Kondo volume-collapse model [17], the semiempirical band model [18] and the Mott transition model [19]. On the other hand, the first-order valence transition in  $\text{EuPd}_2\text{Si}_2$  and  $\text{YbInCu}_4$  was explained using a simple valence-fluctuation model [11, 13].

To investigate anisotropic behaviour of the first-order valence transition in the orthorhombic  $\text{CeNi}_{1-x}\text{Co}_x\text{Sn}$  alloys, we have synthesized a single crystal with starting composition  $\text{CeNi}_{0.62}\text{Co}_{0.38}\text{Sn}$ , which was the best composition found in our previous polycrystalline studies [14]. The electron-probe microanalysis (EPMA) revealed that the Co composition varies along the length of the crystal;  $x = 0.32$  for the top part and  $x = 0.35$  for the bottom part. The magnetic susceptibility measurements reveal a sharp drop in the susceptibility with large thermal hysteresis for the bottom part with  $x = 0.35$ , while no sharp transition was observed for the top part with  $x = 0.32$ . To understand this behaviour, we have also made systematic studies on polycrystalline  $\text{CeNi}_{1-x}\text{Co}_x\text{Sn}$  alloys with  $x = 0.31$  to  $0.38$  in steps of  $0.01$ . The effect of annealing and the results of our x-ray diffraction studies and magnetic susceptibility measurements are discussed in the present paper.

## 2. Experimental details

The single crystal with a starting composition  $\text{CeNi}_{0.62}\text{Co}_{0.38}\text{Sn}$  was grown by a Czochralski method using a radio-frequency induction furnace with a hot tungsten crucible. The details of the growth condition are similar to those used for  $\text{CeNiSn}$  [20]. The purity of starting materials was 99.999% for Ce and Sn (Ce was obtained from Ames Laboratory), 99.99% for Ni and Co. Polycrystalline alloys  $\text{CeNi}_{1-x}\text{Co}_x\text{Sn}$  ( $x = 0.31$ – $0.38$ ) were synthesized by arc melting the constituent elements with purity 99.99% for Ce, Ni and Co and 99.999% for Sn under a high-purity argon atmosphere. To investigate the effect of annealing on the valence phase transition, samples were annealed at  $1000^\circ\text{C}$  for two weeks. Powder x-ray diffraction and magnetic studies were carried out on both as-cast and annealed samples. The compositions of the single crystal and polycrystalline samples were determined by electron-probe microanalysis (EPMA). The single crystal sample has been checked by Laue x-ray diffraction, confirmed to be single crystalline with the growth direction along the  $b$ -axis. The single phase natures of the polycrystalline samples were checked using the x-ray powder diffraction method. The magnetic susceptibility measurements were carried out using a SQUID magnetometer in an applied field of  $0.2\text{ T}$ . The samples mounted inside a plastic capsule were cooled down to  $4\text{ K}$  in zero applied field. Then the data were collected during warming up and cooling down cycles. The ac heat capacity measurements were carried out on a small plate-like sample  $0.11\text{ mm}$  in thickness and  $4.3\text{ mg}$  in weight using an optical ac calorimeter, which was operated at  $3.2\text{ Hz}$  for a chopping frequency of light with a digital lock-in amplifier.

## 3. Results and discussion

EPMA of the single crystal was carried out on both the top part (the part just below the seed) and the bottom part. EPMA of the top part revealed the composition very close to  $\text{CeNi}_{0.68}\text{Co}_{0.32}\text{Sn}$ ,

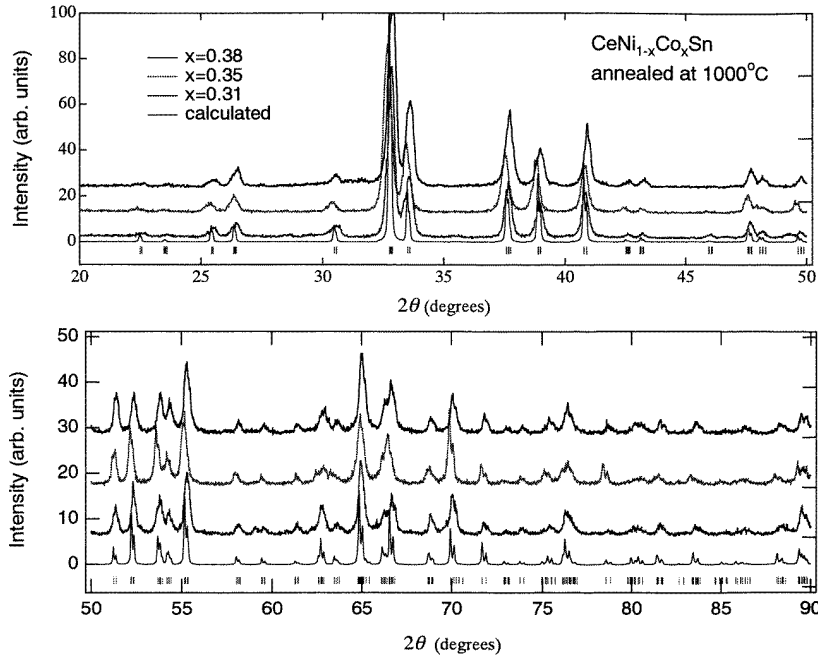


**Figure 1.** Powder x-ray diffraction patterns recorded with Cu  $K\alpha$  radiation for selected annealed alloys of  $CeNi_{1-x}Co_xSn$  at room temperature. The solid line at the bottom represents a simulated powder x-ray diffraction pattern using atomic position parameters determined for  $x = 0.38$  [14]. Note that a valence transition takes place only for  $0.33 \leq x \leq 0.36$  at low temperatures.

while  $CeNi_{0.65}Co_{0.35}Sn$  composition is observed for the bottom part. Both parts were used for the magnetic susceptibility measurements. EPMA on a polycrystalline  $CeNi_{0.65}Co_{0.35}Sn$  alloy showed that the sample was very homogeneous with composition almost same as the starting composition. X-ray powder diffraction studies of polycrystalline as-cast (unannealed) as well as annealed samples showed that all samples were single phase materials and crystallized in the orthorhombic  $TiNiSi$ -type structure. Figure 1 shows the x-ray diffraction pattern for  $x = 0.31, 0.35, 0.38$  (annealed) alloys along with the simulated powder diffraction pattern obtained using the RIETAN94 program. It can be seen from figure 1 that all the observed reflections could be ascribed to the  $TiNiSi$ -type structure, space group  $Pnma$ . It is to be noted that the XRD patterns for the as-cast and annealed samples were almost the same for  $x = 0.31, 0.32, 0.37$  and  $0.38$ . However, for  $x = 0.33$ – $0.35$  alloys noticeable increases in the intensity of a few reflections were observed in the annealed samples compared with as-cast samples: reflection (303) in  $x = 0.33$ , (015) in  $x = 0.33$  and  $0.34$  and (512), (215), (610) in  $x = 0.35$ . At present we do not have a clear explanation for this, but we attribute to the preferred orientation. It is highly possible that with annealing the crystallographic ordering takes place between Ni and Co atoms. The orthorhombic space groups  $Pnm2_1$  and  $P2_1ma$  are compatible with preferential occupancy of different Ni and Co sites. However, at present we do not have any clear evidence for this. The room-temperature lattice parameters estimated using the CELL program and taking into account the positions of lines are given in figure 2. We noted for  $x = 0.31$ – $0.35$  alloys the value of  $a$  is slightly larger than that of  $c$  for all alloys, which is in contrast to the pure  $CeNiSn$  in which lattice parameter  $c$  ( $= 7.617 \text{ \AA}$ ) is larger than  $a$  ( $= 7.542 \text{ \AA}$ ). This suggests that the lattice parameters  $a$  and  $c$  cross each other at some

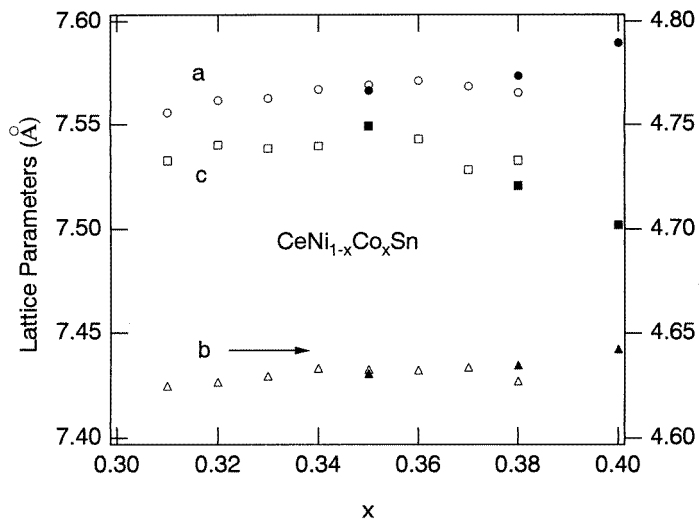


**Figure 2.** Lattice parameters versus Co concentration  $x$  for  $\text{CeNi}_{1-x}\text{Co}_x\text{Sn}$  alloys. Solid symbols represent lattice parameters estimated from neutron diffraction studies [14, 21].

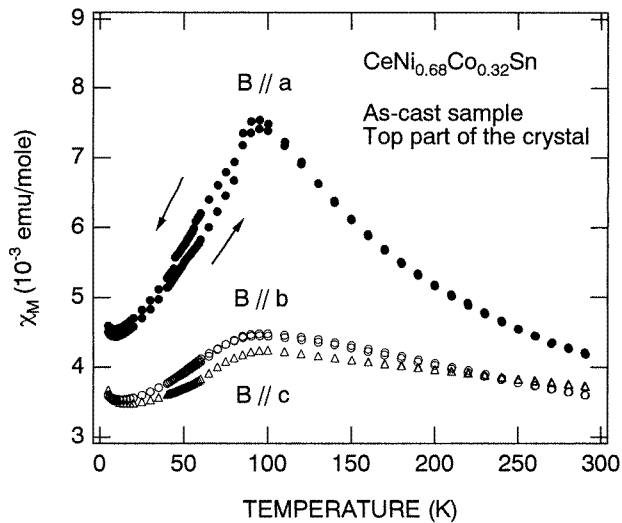


**Figure 3.** Magnetic susceptibility versus temperature for the as-grown single crystal  $\text{CeNi}_{0.68}\text{Co}_{0.32}\text{Sn}$  for  $B \parallel a$ ,  $B \parallel b$  and  $B \parallel c$ .

intermediate composition. The unit-cell volume increases gradually from  $V = 263.219 \text{ \AA}^3$  for  $x = 0.31$  to  $V = 264.706 \text{ \AA}^3$  for  $x = 0.35$ . This might suggest a slight decrease in the Ce valence (at high temperatures) with increasing  $x$  from 0.31 to 0.35, which is in corroboration with magnetic susceptibility measurements discussed below. Further, it is to be noted that the unit-cell volume  $V = 264.326 \text{ \AA}^3$  for  $x = 0.34$  alloys is very close to  $V = 264.310 \text{ \AA}^3$  for the host  $\text{CeNiSn}$ .

Figure 3 shows the magnetic susceptibility of the as-cast single crystal  $\text{CeNi}_{0.68}\text{Co}_{0.32}\text{Sn}$  along the three principal axes. The magnetic susceptibility exhibits a highly anisotropic

behaviour with easy  $a$ -axis magnetization:  $\chi_a > \chi_b \geq \chi_c$ . The anisotropic behaviour observed in the susceptibility is almost similar to that observed in the host CeNiSn [22]. The susceptibility along the  $a$ -axis exhibits a peak at 100 K (figure 3). The origin of the peak in  $\chi_a(T)$  in the present alloy and in host CeNiSn is different, the peak in the former arising due to the anisotropic valence fluctuation behaviour, while in the latter it arises due to the gap formation at the Fermi level. Further, the absolute value of  $\chi_a$  (100 K) for CeNi<sub>0.68</sub>Co<sub>0.32</sub>Sn is larger than that of CeNiSn. A small hysteresis was observed in the susceptibility between warming up and cooling down data below 100 K; however, it was not as large as observed in our previous and present polycrystalline samples [14]. We have also measured the magnetic susceptibility of the annealed (at 1000 °C for two weeks) single crystal, which shows almost the same behaviour as observed for the as-cast one. However, we noticed two differences: (1) no hysteresis was observed between warming up and cooling down data and the peak at 100 K was broadened, and (2) a small increase in the anisotropy between  $b$  and  $c$  axes,  $\chi_b > \chi_c$  up to room temperature and slight increase in the absolute values for all three directions.

The absence of the clear hysteresis in  $\chi$  for the single crystal CeNi<sub>0.68</sub>Co<sub>0.32</sub>Sn is consistent with our measurements on polycrystalline samples. We have observed a valence fluctuation behaviour in the polycrystalline samples in the past and the present studies [14]. The anisotropic behaviour of the magnetic susceptibility could be understood by considering the effect of crystalline electric fields and anisotropic hybridization between the 4f and conduction electrons in the orthorhombic structure. The latter gives anisotropic Kondo effect even in a valence fluctuating system, as was observed in a hexagonal compound CeNiIn [23].

Figure 4(a) shows the magnetic susceptibility of the annealed single crystal CeNi<sub>0.65</sub>Co<sub>0.35</sub>Sn for  $B\parallel a$  and  $B\parallel c$  down to 5 K. For  $B\parallel a$  the magnetic susceptibility exhibits a sharp drop at 50 K and large thermal hysteresis ( $\Delta T = 25$  K), indicating the first-order transition. It is to be noted that after one cycle of measurements (i.e. cooling, heating and cooling) the crystal was broken into many pieces (became almost like powder). The breaking of the crystal is due to anisotropic thermal expansion at the valence transition ( $T_V$ ): lattice parameters  $a$  and  $b$  decrease, while  $c$  increases at  $T_V$  [14, 21]. Hence for  $B\parallel c$  measurements another piece of the crystal was used. This piece was also broken in many pieces after  $B\parallel c$  measurements. Therefore the data for  $B\parallel c$  might not be reliable as there may be a contribution coming from the easy axis (i.e.,  $B\parallel a$ ) due to partial alignment of powder along the applied field. Nevertheless, we can see the valence transition for both  $B\parallel a$  and  $B\parallel c$ .

Because of the breaking of the crystal it was not possible to study anisotropy below  $T_V$ . To investigate the anisotropy above  $T_V$ , we have measured  $\chi(T)$  on a third piece of the single crystal between 80 and 300 K. For this temperature range the crystal was not broken, hence we could measure  $\chi_a(T)$ ,  $\chi_b(T)$  and  $\chi_c(T)$  on the same piece of the crystal (figure 4(b)). It is clear from figure 4(b) that the susceptibility exhibits a strong anisotropic behaviour with easy  $a$ -axis.  $\chi_a(T)$  is strongly temperature dependent, while  $\chi_b(T)$  and  $\chi_c(T)$  are almost temperature independent between 80 and 300 K. The plot of  $\chi_a^{-1}$  versus  $T$  (not shown here) does not follow the Curie–Weiss (C–W) law; instead it exhibits a strong curvature. We found that the results of  $\chi_a(T)$  above  $T_V$  can be fitted well with a modified C–W law;  $\chi(T) = C/(T - \theta_p) + \chi_p$ , where  $C$  is the Curie constant,  $\theta_p$  is the paramagnetic Curie temperature and  $\chi_p$  is the temperature independent Pauli susceptibility; solid lines in figures 4(a) and 4(b) represent the fit. The fit gives the effective magnetic moment,  $\mu_{eff} = 2.72 \mu_B$ ,  $\theta_p = -4$  K and  $\chi_p = 3.75 \times 10^{-3}$  emu mol<sup>-1</sup>. The observed  $\mu_{eff}$  value is larger than the value  $2.54 \mu_B$  expected for the free Ce<sup>3+</sup> ions with  $J = 5/2$ , and the value of  $\chi_p$  is higher than that observed in CeNiSn and other Ce<sup>3+</sup> compounds.

Next we discuss the annealing effects on the susceptibility for polycrystalline CeNi<sub>1-x</sub>Co<sub>x</sub>Sn alloys. It is to be noted that the results of  $x = 0.31, 0.32$  and  $0.38$  alloys do

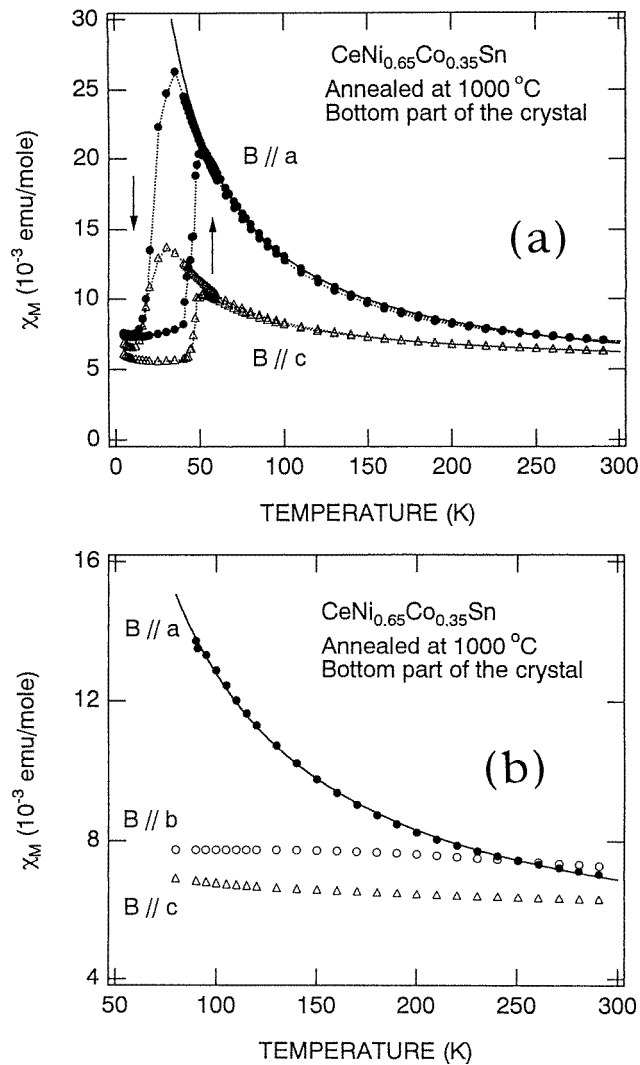


**Figure 4.** Magnetic susceptibility versus temperature for the annealed single crystal  $\text{CeNi}_{0.65}\text{Co}_{0.35}\text{Sn}$  for  $B // a$ ,  $B // b$  and  $B // c$ : (a) temperature range between 4.2 and 300 K and (b) temperature range between 80 and 300 K. The solid line represents a fit to modified C–W behaviour. Dotted lines are guides to the eye.

not change much with annealing. However,  $\chi(T)$  of  $x = 0.33$ – $0.37$  alloys exhibits a dramatic change in the behaviour with annealing: for comparison see figure 5 for  $x = 0.31$  and  $0.35$ . The high absolute values and weak temperature dependent susceptibility for the as-cast alloys with  $x = 0.33$ – $0.37$  are unusual and do not have any clear explanation. However, we believe that three factors that might give this behaviour: (1) internal stresses, (2) disorder between Co and Ni atoms and (3) a small amount of unreacted Ni or Co impurities; EPMA did not show any evidence for segregation of free Co and Ni.  $\chi(T)$  of  $x = 0.31$  and  $0.32$  alloys exhibits a weak temperature dependent behaviour and a maximum between 90 and 100 K. This behaviour indicates that the Ce ions are in a valence fluctuating state in these alloys. The values of

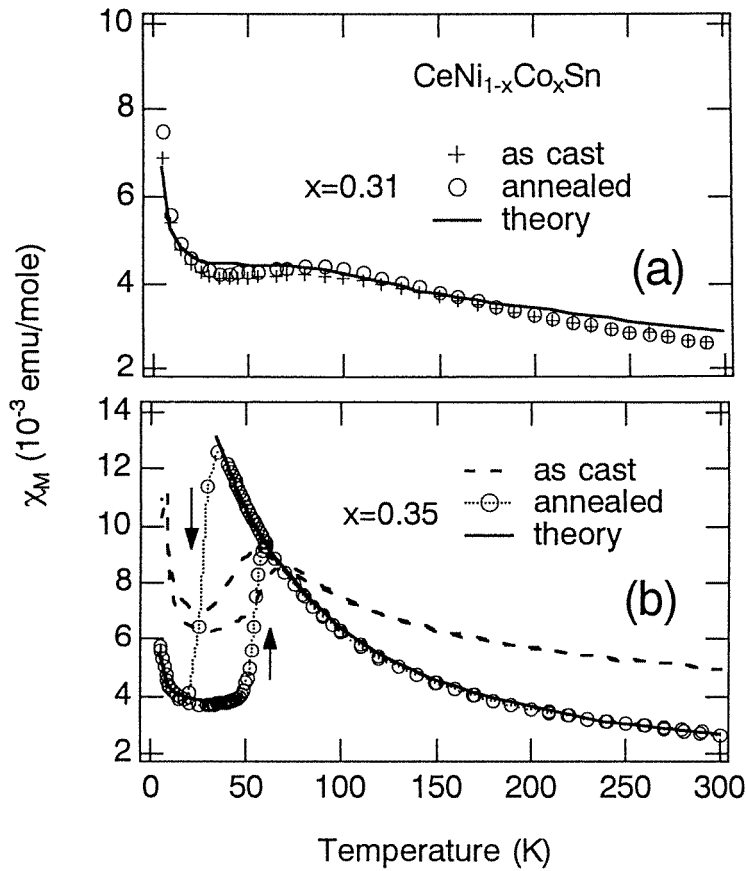


**Figure 5.** Magnetic susceptibility versus temperature for  $CeNi_{1-x}Co_xSn$  alloys, as cast and annealed: (a) for  $x = 0.31$  alloy and (b) for  $x = 0.35$  alloy. Solid lines represent the fit, see text.

$\mu_{eff}$  and  $\theta_p$  obtained from C–W behaviour between 150 and 300 K are:  $\mu_{eff} = 3.1 \mu_B$  and  $\theta_p = -165$  K for  $x = 0.31$  and  $\mu_{eff} = 3.1 \mu_B$  and  $\theta_p = -107$  K for  $x = 0.32$ . It is to be noted that slightly higher values of  $\mu_{eff}$  and  $|\theta_p|$  were observed in as-cast samples.

The susceptibility of annealed alloys with  $x = 0.33$ – $0.36$  shows a sharp drop and large thermal hysteresis between 30 and 70 K (figures 5 and 6). This hysteresis confirms the first-order nature of the transition in these alloys. A very similar behaviour has been observed in  $YbInCu_4$  [13] and Ce metal [8], which also exhibit a first-order valence transition. The as-cast  $x = 0.37$  alloy exhibits a sharp drop in  $\chi(T)$  at 40 K, which almost disappeared in the annealed sample. For  $x = 0.38$   $\chi(T)$  exhibits normal Curie–Weiss behaviour between 100 and 300 K, with  $\mu_{eff} = 3.0 \mu_B$  and  $\theta_p = -109$  K, but deviates considerably from it below 100 K. The observed values of  $\mu_{eff}$  in  $x = 0.31$ ,  $0.32$  and  $0.38$  alloys are higher than  $2.54 \mu_B$ , the value for free  $Ce^{3+}$  ions. We noted that the high temperature susceptibility of the alloys exhibiting the valence transition does not follow well defined C–W behaviour, but instead shows a modified C–W law with  $\mu_{eff} = 2.25 \mu_B$ ,  $\theta_p = -12$  K and  $\chi_p = 0.6 \times 10^{-3} \text{ emu mol}^{-1}$  for  $x = 0.35$ . It is possible that the observed deviation from the C–W law in these alloys could arise from the crystalline electric field effect as inferred from neutron scattering experiments [14].



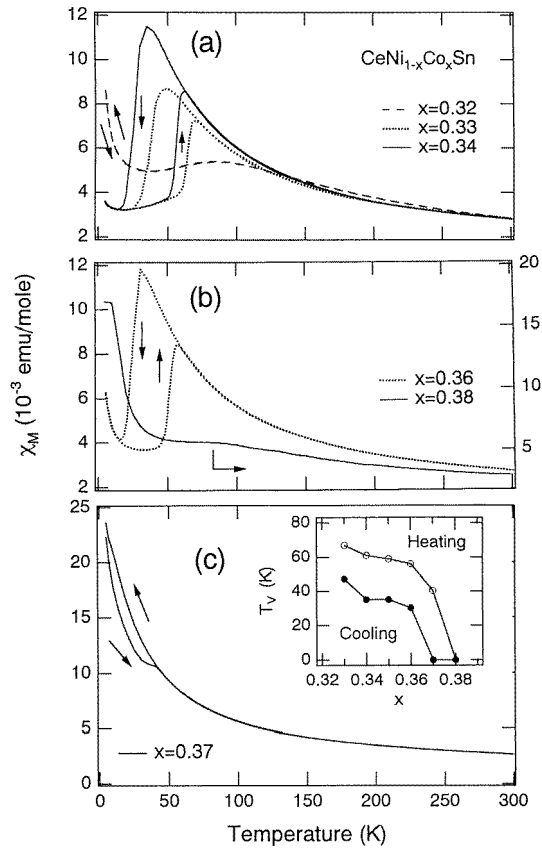


**Figure 6.** Magnetic susceptibility of annealed polycrystalline  $\text{CeNi}_{1-x}\text{Co}_x\text{Sn}$  alloys ( $x = 0.32$  to  $0.38$ ): (a) for  $x = 0.32, 0.33$  and  $0.34$  alloys, (b) for  $x = 0.36$  and  $0.38$  alloys and (c) for  $x = 0.37$  alloy. The inset shows valence transition temperature ( $T_V$ ) versus Co composition ( $x$ ).

The observed temperature dependence of the susceptibility of the  $x = 0.31$  alloy has been analysed on the basis of the Coqblin–Schrieffer (C–S) model [24]. The model takes into account impurity mediated hopping of the conduction electrons between various eigenstates of  $J$ , where  $J$  is the total angular momentum of the impurity: for  $\text{Ce}^{3+}$   $J = 5/2$ . On the basis of the Bethe *ansatz* solution of the C–S Hamiltonian, Rajan has calculated the temperature dependent impurity susceptibility for  $J = 1/2$  to  $7/2$  [25]. The model is based on a single parameter, a characteristic temperature  $T_0$ , which is related to the Kondo temperature  $T_K$  through the Wilson number,  $T_K = WT_0$ . The details of this model and analysis presented here are given in [25, 26]. In the present analysis we have used Rajan’s theoretical impurity susceptibility curve for  $J = 5/2$ . In order to account for the low temperature rise in the susceptibility, an impurity term  $nC/T$  (where  $n$  is the impurity concentration and  $C$  the Curie constant of the free  $\text{Ce}^{3+}$  ion) was included in the analysis. The temperature independent susceptibility  $\chi_p$ , arising from conduction electron Pauli paramagnetism, was also included in the analysis. The value of parameters obtained from a least squares fit to the susceptibility data of  $x = 0.31$  alloy are  $T_0 = 270$  K,  $n = 0.017$  and  $\chi_p = 0.001$  ( $\text{emu mol}^{-1}$ ). The quality of the fit may be seen from the calculated susceptibility as shown by the solid line in figure 5(a).

We now turn to the model to describe a first-order valence transition. The first-order valence transition in  $Ce_{0.7}Th_{0.3}$  has been analysed by introducing the volume dependence of the Kondo coupling constant  $J_{sf}$  and using the universal impurity susceptibility curve for  $J = 5/2$  [27]. As the volume changes with temperature, one can write the temperature dependence of  $T_K(T) = D \exp(-1/J_{sf}) = D \exp(-1/(a + bV(T)/V_0))$ , where  $D$  is the conduction bandwidth,  $a$  and  $b$  are variables and  $V_0$  is the reference volume. This procedure gave good agreement between experimental and calculated susceptibility of  $Ce_{0.7}Th_{0.3}$  [27]. Therefore, we tried to analyse the susceptibility data of  $x = 0.35$  on the basis of the above method and using experimental data of  $V(T)$  for  $x = 0.38$  alloy [14]. The present analysis shows that 0.3% decrease in volume at  $T_V$  gives a small increase in  $T_K$  ( $\Delta T_K/T_K = 2.3\%$ ) at  $T_V$ . However, this increase in  $T_K$  was not enough to reproduce the observed 69% drop in the susceptibility at  $T_V$  for  $x = 0.35$  alloy.

Thus, to estimate the characteristic energy of the high-temperature phase and the low-temperature phase independently, we have analysed the  $\chi(T)$  data of  $x = 0.35$  alloy in two temperature regimes separately by using a method similar to that used for  $x = 0.31$  alloy mentioned above. However, for the high-temperature phase, in which crystal-field excitations have been observed [14], the model may not be appropriate. Nevertheless, we will use this model to obtain some idea about the characteristic energy. First we analysed the low-temperature data and estimated the values of  $n$  and  $\chi_p$ , which were kept fixed for the analysis of high-temperature data. The value of the parameters obtained from the least-squares fit are:  $T_{0low} = 280$  K,  $n = 0.004$ ,  $\chi_p = 0.22 \times 10^{-3}$  (emu mol $^{-1}$ ) and  $T_{0high} = 40$  K. The solid lines in figure 5(b) represent the fit. This indicates that the characteristic energy increases about sixfold below  $T_V$ . A similarly large increase in the characteristic energy of the low-temperature phase has also been reported for Ce metal and YbInCu $_4$  [8, 28].

To examine the first-order transition, we have measured the heat capacity for the annealed polycrystalline sample with the optimum composition  $x = 0.35$ . Figure 7 shows the ac heat capacity versus temperature; the inset shows the data near the transition obtained during the heating cycle. We observed a distinct peak in the heat capacity at the same temperature where susceptibility exhibits a large jump. A very similar behaviour has been observed in the heat capacity of polycrystalline YbInCu $_4$  [29, 30]. On the other hand, the heat capacity of YbInCu $_4$  single crystals exhibits a first-order type anomaly at  $T_V$  along with a jump in the entropy of 10 J mol $^{-1}$  K $^{-1}$  [31]. The second-order-type anomaly in our data shown in figure 7 may be ascribed to lattice defects and small stoichiometric variation throughout the sample. For the first-order transition the entropy should exhibit a discontinuity at the transition. However, from the present ac heat capacity measurements it was not possible to calculate the entropy. Detailed dc heat capacity measurements on CeNi $_{0.65}$ Co $_{0.35}$ Sn single crystal and the reference LaNi $_{0.65}$ Co $_{0.34}$ Sn are required to evaluate the change in the entropy at  $T_V$ .

To understand the mechanism responsible for the phase transition in CeNi $_{0.65}$ Co $_{0.35}$ Sn, we compare the change in the Kondo temperature ( $\Delta T_K/T_K$ ) and that in the volume ( $\Delta V/V$ ) at transition with those for the  $\alpha \rightarrow \gamma$  transition in Ce metal and YbInCu $_4$ :  $\Delta T_K/T_K = -\Omega \Delta V/V$ , where  $\Omega$  is the Grüneisen parameter [32]. For the  $\alpha \rightarrow \gamma$  transition  $\Delta T_K/T_K = 8.6$  and  $\Delta V/V = -0.2$ , this gives  $\Omega = 43$ , in agreement with the experimentally observed value 25.2 [8]. This confirms that the Kondo volume collapse (KVC) model is appropriate to the  $\alpha \rightarrow \gamma$  phase transition in Ce metal. However, such an analysis for YbInCu $_4$  gives  $\Omega = 4000$  ( $\Delta T_K/T_K = 20$  and  $\Delta V/V = 0.005$ ), which is two orders of magnitude larger than the experimental value of 55 [32]. Now if we apply similar analysis to CeNi $_{0.65}$ Co $_{0.35}$ Sn with  $T_{0low} = 280$  K and  $T_{0high} = 40$  K,  $\Delta T_K/T_K = 6$  (11.2, from inelastic neutron scattering linewidths for  $x = 0.38$  [14]) and  $\Delta V/V = -0.003$  [14], we obtain  $\Omega = 2000$  (3733). This value of  $\Omega$  is unrealistically large. At present the experimental value of  $\Omega$  is not available for

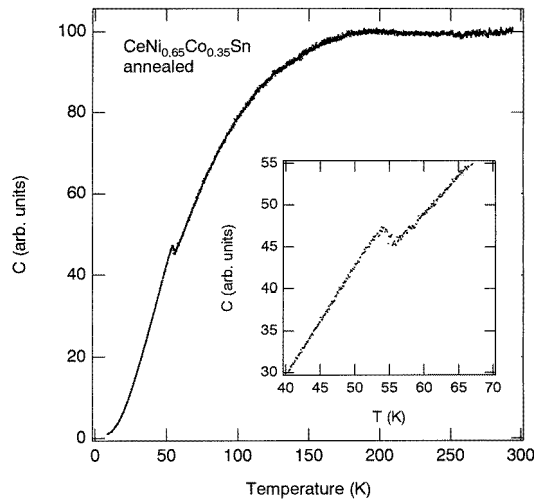


**Figure 7.** Ac heat capacity versus temperature for an annealed polycrystalline  $\text{CeNi}_{0.65}\text{Co}_{0.35}\text{Sn}$  alloy; the inset shows the behaviour near the transition.

$\text{CeNi}_{0.65}\text{Co}_{0.35}\text{Sn}$ . Recalling that  $T_V$  and  $\Delta V/V$  for  $\text{CeNi}_{0.65}\text{Co}_{0.35}\text{Sn}$  are almost the same as for  $\text{YbInCu}_4$ , we assume the value of  $\Omega = 55$  as in  $\text{YbInCu}_4$ . Then, we obtain  $\Delta V/V = -0.1$  ( $-0.2$ ) for the observed  $\Delta T_K/T_K = 6$  ( $11.2$ ), which is much larger than the actually observed value  $-0.003$ . Thus the observed small discontinuity in volume simply cannot generate the large change in  $T_K$  observed at the valence transition in  $\text{CeNi}_{1-x}\text{Co}_x\text{Sn}$  alloys. This suggests that the Kondo volume collapse model can not be applied to the valence phase transition in this system. A possible mechanism responsible for the valence phase transition should produce a large change in  $T_K$  with a small volume change at  $T_V$ . This may be possible with fine tuning of the position of the Fermi level, which results in a large increase in the hybridization and hence  $T_K$  with small change in unit cell volume. A similar interpretation has been given to the valence phase transition in  $\text{YbInCu}_4$  [28, 32].

#### 4. Conclusions

We have synthesized and studied the magnetic susceptibility of single crystals  $\text{CeNi}_{0.68}\text{Co}_{0.32}\text{Sn}$  and  $\text{CeNi}_{0.65}\text{Co}_{0.35}\text{Sn}$ . The magnetic susceptibility for  $x = 0.32$  reveals that the Ce ions are in a valence fluctuating state with a strongly anisotropic Kondo effect which comes from anisotropic hybridization in the  $k$ -space of the orthorhombic structure. A sharp first-order valence transition has been observed for the crystal with  $x = 0.35$ . For polycrystalline samples, in the narrow range of Co composition  $0.33 \leq x \leq 0.36$ , the transition becomes sharper by annealing at  $1000^\circ\text{C}$ , even though the room temperature x-ray diffraction patterns are almost identical. The present studies show that the first-order transition is very sensitive to the Co concentration and the highest transition temperature of 67 K has been observed for the annealed sample with  $x = 0.33$ . For  $x = 0.33$ , out of the six Ce–Ni/Co bond lengths two have shorter (Ce–Ni) bond lengths than the other four. Thus it is possible that the Co atoms preferentially occupy these sites, yielding a stoichiometric compound  $\text{Ce}_3\text{Ni}_2\text{CoSn}_3$ . Neutron diffraction studies on annealed samples are required to solve this structural problem. We have presented the analysis of the magnetic susceptibility of the alloy exhibiting valence fluctuating

behaviour. An attempt has been made to estimate the Kondo temperature for both the low- and high-temperature phases for the alloy that shows the first-order valence transition. A large change in the Kondo temperature ( $\Delta T_K/T_K = 11.2$ ) along with a small change in the volume ( $\Delta V/V = -0.003$ ) at the transition suggests that the Kondo volume collapse model cannot be applied to the present alloy system. We have discussed a possible mechanism responsible for the valence phase transition in  $CeNi_{1-x}Co_xSn$  alloys.

### Acknowledgments

We would like to thank Y Shibata, the Instrument Centre for Chemical Analysis, for EPMA, and Professor F Iga for help in susceptibility measurements and valuable discussions. One of us (DTA) is thankful to the Japan Society for the Promotion of Science (JSPS) for the award of a research fellowship.

### References

- [1] Wohlflehen D K and Coles B R 1973 *Magnetism* vol 5, ed H Suhl (New York: Academic) p 3
- [2] See, for example, Wachter P and Boppert H (eds) 1982 *Valence Instabilities* (Amsterdam: North-Holland)
- [3] Vijayaraghavan R 1985 *J. Magn. Magn. Mater.* **47/48** 561
- [4] Adroja D T, Malik S K, Padalia B D and Vijayaraghavan R 1989 *Phys. Rev. B* **39** 4831
- [5] Adroja D T, Malik S K, Padalia B D, Bhatia S N, Walia R and Vijayaraghavan R 1990 *Phys. Rev. B* **42** 2700
- [6] De Teresa J M, Arnold Z, del Moral A, Ibarra M R, Kamarád J, Adroja D T and Rainford B D 1996 *Solid State Commun.* **99** 911
- [7] Adroja D T, Rainford B D and Jansen A G M 1995 *J. Magn. Magn. Mater.* **140–144** 1217
- [8] Naka T, Matsumoto T and Mori N 1995 *Physica B* **205** 121
- [9] Gignoux D and Voiron J 1985 *Phys. Rev. B* **32** 4822
- [10] Jayaraman A 1979 *Handbook on the Physics and Chemistry of Rare Earths* ed K A Gschneider Jr and L Eyring (Amsterdam: North Holland)
- [11] Croft M, Hodges J A, Kemly E, Krishnan A, Murgai V and Gupta L C 1982 *Phys. Rev. Lett.* **48** 826
- [12] Michels G, Huhnt C, Scharbrodt W, Schlabitiz W, Holland-Moritz E, Abd-Elmeguid M M, Micklitz H, Johrendt D and Keimes V 1995 *Z. Phys. B* **98** 75
- [13] Felner I and Nowik I 1986 *Phys. Rev. B* **32** 617
- [14] Adroja D T, Rainford B D, Teresa J M De, del Moral A, Ibarra M R and Knight K S 1995 *Phys. Rev. B* **52** 12 790  
Adroja D T and Rainford B D 1998 unpublished
- [15] Shapiro S M, Axe J D, Birgeneau R J, Lawrence J M and Parks R D 1977 *Phys. Rev. B* **16** 2225
- [16] Zachariasen W H, as quoted by Lawson A W and Tang T Y 1949 *Phys. Rev.* **76** 301  
Pauling L, as quoted by Schuch A F and Sturdivant J H 1950 *J. Chem. Phys.* **18** 145
- [17] Allen J W and Martin R M 1982 *Phys. Rev. Lett.* **49** 1106  
Allen J W and Liu L Z 1992 *Phys. Rev. B* **46** 5047
- [18] Rainford B D and Edwards D M 1987 *J. Magn. Magn. Mater.* **63/64** 557
- [19] Johansson B, Abrikosov I A, Alden M, Ruban A V and Skiver H L 1995 *Phys. Rev. Lett.* **74** 2335
- [20] Nakamoto G, Takabatake T, Bando Y, Fujii H, Izawa K, Suzuki T, Fujita T, Minami A, Oguro I, Tai L T and Menovsky A A 1995 *Physica B* **206/207** 840  
Nakamoto G, Takabatake T, Fujii H, Minami A, Maezawa K, Oguro I and Menovsky A A 1995 *J. Phys. Soc. Japan* **64** 4837
- [21] De Teresa J M, Adroja D T, Rainford B D, Knight K S, del Moral A and Ibarra M R 1997 *Physica B* **234–236** 872
- [22] Takabatake T *et al* 1993 *Transport and Thermal Properties of f-Electron Systems* ed G Oomi *et al* (New York: Plenum) p 1
- [23] Fujii H, Inoue T, Andoh Y, Takabatake T, Satoh K, Maeno Y, Fujita T, Sakurai J and Yamaguchi Y 1989 *Phys. Rev. B* **39** 6840
- [24] Coqblin B and Schrieffer J R 1969 *Phys. Rev.* **185** 847
- [25] Rajan V T 1983 *Phys. Rev. Lett.* **51** 308
- [26] Adroja D T and Rainford B D 1993 *J. Magn. Magn. Mater.* **119** 54
- [27] Allen J W, Kang J S and Oh S J 1987 *J. Magn. Magn. Mater.* **63/64** 515

- [28] Sarrao J L, Immer C D, Benton C I, Fisk Z, Lawrence J M, Mandrus D and Thompson J D 1996 *Phys. Rev. B* **54** 12 207
- [29] Felner I *et al* 1987 *Phys. Rev. B* **35** 6956
- [30] Hauser R, Naber L, Schaudy G, Bauer E, Hilscher G, Kindle B and Assmus W 1996 *Czech. J. Phys.* **46** 2543
- [31] Sarrao J L, Ramirez A P, Darling T W, Freibert F, Migliori A, Immer C D, Fisk Z and Uwatoko Y 1998 *Phys. Rev. B* **58** 409
- [32] Cornelius A L, Lawrence J M, Sarrao J L, Fisk Z, Hundley M F, Kwei G H, Thompson J D, Booth C H and Bridges F 1997 *Phys. Rev. B* **56** 7993